

Model for creep failure with healing

Subhadeep Roy^{1,*} and Takahiro Hatano^{2,†}

¹*PoreLab, Department of Physics, Norwegian University of Science and Technology, NO7491 Trondheim, Norway*

²*Department of Earth and Space Science, Osaka University, 560-0043 Osaka, Japan*



(Received 17 February 2022; accepted 8 March 2022; published 10 May 2022)

To understand general properties of creep failure with healing effects, we study a mean-field fiber bundle model with probabilistic rupture and rejoining processes. The dynamics of the model is determined by two factors: bond breaking and formation of new bonds. Steady states are realized due to the balance between breaking and healing beyond a critical healing factor, below which the bundle breaks completely. Correlation between the fluctuating value of strain generated in the model with time at the steady state leads to a characteristic time that diverges in a scale-free manner as we approach the critical healing factor. Transient behaviors in the strain rate also involve a power law with a nonuniversal exponent.

DOI: [10.1103/PhysRevResearch.4.023110](https://doi.org/10.1103/PhysRevResearch.4.023110)

I. INTRODUCTION

Fracture phenomena in disordered systems constitute an important problem in various contexts such as industries, mechanical engineering, materials science, earth and planetary science, and statistical physics [1,2]. Historically, statistical physics has aimed at the competition between two kinds of randomness: thermal fluctuation and structural disorder. This problem is also important in fracture phenomena: how the failure dynamics is affected by the structural randomness and temperature.

Generally, rupture dynamics is sensitive to temperature. At low temperatures, materials fail immediately if the applied stress reaches the critical value [3]. This is referred to as brittle failure. In contrast, enduring slow deformation precedes rupture at moderate or high temperatures. The latter failure mode is referred to as creep failure [4,5]. Note that creep failure occurs at the stress lower than the critical value.

Due to its enduring nature, creep failure may be accompanied by healing. This is unlikely for open cracks under tensile stress conditions, but more likely for shear failure, where cracks are still in contact after failure. Since healing processes can be also sensitive to temperature, failure dynamics with a healing process provides us with an intriguing problem from the viewpoint of statistical physics.

A phenomenon in which healing plays a vital role is friction, where the protrusions of two surfaces are jointed. Friction force is supported by these jointed protrusions, which are referred to as asperities [6]. The asperities are detached and rejoined repeatedly by the slip motion, which may be regarded as failure and healing, respectively. Another interest-

ing phenomenon is the shear failure of snow, i.e., avalanches. In general, snow is a highly disordered porous material that can heal and thus exhibits a rich response to external stress [7]. Although these phenomena are so complex and involve various elementary physical processes, simple model studies may be useful for extracting and understanding their essential mechanisms.

In this paper, we consider the effect of healing on the dynamics of shear deformation and the subsequent failure by proposing a simple stochastic model. The model we have adopted here is a variation of the fiber bundle model (FBM) [8–10]. Due to its simplicity, the model allows various kinds of extension and thus has been widely utilized to analyze the failure of disordered materials. For instance, although the original FBM does not explicitly include the effect of temperature, there have been some attempts to extend the model to study thermally induced failures [11–15] or noise-induced failures [16–20], in which the effect of temperature is naturally incorporated.

As opposed to the conventional model, these extended models with finite temperature evolve at a constant external load and therefore exhibit rich dynamic behaviors. In particular, a model for snow avalanche has been proposed making use of the FBM [21]. Along the line of these studies, we further extend the FBM to include the healing process. We discuss the time evolution of the model as well as its statistical nature of fluctuations.

In the next section, we explain the conventional fiber bundle model, the algorithms for probabilistic rupture and healing. In Sec. III, we present the numerical results, followed by discussions on the work and the concluding remarks in Sec. IV.

II. DESCRIPTION OF THE MODEL

A. Outline

The model investigated here is analogous to the equal-load sharing fiber bundle model, but here we have made some

*subhadeeproy03@gmail.com

†hatano@ess.sci.osaka-u.ac.jp

Published by the American Physical Society under the terms of the Creative Commons Attribution 4.0 International license. Further distribution of this work must maintain attribution to the author(s) and the published article's title, journal citation, and DOI.

modifications. Below we explain the model, starting with the features common to the conventional one.

Initially, the model consists of N Hookean fibers connected in between two parallel rigid bars, at which the external force F is applied. The force F is redistributed among the constituent fibers. In the equal-load sharing model, which the present study involves, the force F is equally distributed to all the remaining fibers. Namely, the force on each fiber is F/N , which is hereafter referred to as the initial stress, $\sigma_0 := F/N$. Note that this is one of the important parameters in this model.

During time evolution, some fibers may break and thus cannot support the load. Writing the number of intact fibers at time t as L_t , hereafter we use the intact fraction ϕ_t defined by $\phi_t := L_t/N$. The stress at time t , denoted by $\sigma(t)$, is then equal to σ_0/ϕ_t .

B. Fiber strength

The fibers may break under the stress. Each fiber has its own failure strength, which is drawn randomly from the distribution function $\rho(h)$. Although it is difficult to determine the distribution function in experiments, the fracture strength of microelements may not be distributed over several orders of magnitude. We may thus approximate such distribution using a uniform distribution with the mean of $\bar{\sigma}$ and the half-width of δ :

$$\rho(h) = \begin{cases} \frac{1}{2\delta} & (\bar{\sigma} - \delta \leq h \leq \bar{\sigma} + \delta), \\ 0 & (\text{otherwise}). \end{cases} \quad (1)$$

The half-width of distribution, δ , is the measure of disorder in this model.

C. Probabilistic failure

In the conventional model, any fiber breaks once the stress exceeds its threshold value. This process is deterministic. In contrast, in the present model, the rupture criterion of each fiber is probabilistic. We introduce the following function for the rupture probability per unit time for fiber i at time t :

$$P_r(t, i) = k_1 e^{-E(t, i)/k_B T}, \quad (2)$$

where k_1 is the rate constant and $E(i, t)$ is an activation energy for the rupture of fiber i at time t . This is written, using the shear modulus G and the volume constant Ω , as

$$E(t, i) = \frac{\Omega}{2G} [h(i)^2 - \sigma(t)^2], \quad (3)$$

where $h(i)$ and $\sigma(t)$ are, respectively, the strength of fiber i and the stress at time t . If $h(i) \leq \sigma(t)$, fiber i breaks with probability 1 irrespective of Eq. (2).

D. Probabilistic healing

Another important difference from the conventional model is the healing process. Namely, broken fibers can rejoin with a certain probability. During unit time, a broken fiber can heal up at the probability of $P_h(t)$,

$$P_h(t) = k_2 (1 - \phi_t) e^{-A/k_B T}, \quad (4)$$

where k_2 is another rate constant, A is an activation energy for healing, and ϕ_t is the fraction of intact fibers at time t : $\phi_t = L_t/N$.

The factor of $(1 - \phi_t)$ in Eq. (4) means that the healing probability of a single broken fiber is proportional to the number of broken fibers. This implies that healing can occur when a broken fiber meets another broken one. In this respect, the rate constant k_2 may be interpreted as the collision frequency of broken fibers. This further suggests that k_2 may be proportional to the slip velocity or shear rate, since the collision frequency of fibers is generally proportional to the slip velocity for shear deformation. The healing probability is large when the shear rate is large, since there are more chances for a broken fiber to be in contact with other broken ones. In the context of friction, this is the frequency at which a protrusion meets another. It is thus proportional to the slip velocity.

We can rewrite the healing probability in a simpler manner,

$$P_h(t) = \omega(1 - \phi_t), \quad (5)$$

with $\omega := k_2 \exp(-A/k_B T)$. The independent parameters are then reduced from (k_2, A) to ω . The intrinsic rate constants are thus (k_1, ω) . Note that ω depends on the temperature, while k_1 does not.

A rejoined fiber is assigned a new strength (threshold stress) according to the distribution function given by Eq. (1). We assume that a certain fiber is allowed to rejoin infinite times.

E. Time evolution

Although the conventional FBM does not have the concept of time, there have been some attempts to extend the model to describe time evolution [11,14]. The basic idea is to introduce the duration required for the stress redistribution. More precisely, the rupture of a single fiber and the subsequent stress redistribution may take a certain time. This duration is denoted by τ , which is an intrinsic timescale in the model. The time evolution of the present system thus consists of the accumulation of this intrinsic timescale: $t \rightarrow t + \tau$. Namely, τ constitutes a single time step. Since τ is an intrinsic time constant, the time evolution here is inherently discrete and we cannot consider the continuous limit: $\tau \rightarrow 0$.

During this single time step, the rupture probability for an intact fiber is $\tau P_r(t)$, and the healing probability for a broken fiber is $\tau P_h(t)$.

At $t = 0$, the force on each fiber is σ_0 . The failure probability per unit time $P_r(0, i)$ is then computed for each fiber using Eqs. (2) and (3). A random number $R(0, i)$ is drawn from the uniform distribution defined on the interval $[0,1]$. If $R(0, i) < \tau P_r(0, i)$, fiber i breaks and is removed in the next time step ($t = \tau$). This process is repeated for all the fibers.

In the subsequent time steps ($t \geq \tau$), all the fibers are inspected in order: $i = 1, 2, \dots, N$. If fiber i is intact, the above procedure is repeated to check if it fails or not. If fiber i is broken, we check if it heals or not. This is done by drawing another random number $R^*(t, i)$ from the uniform distribution on $[0,1]$. If $R^*(t, i) < \tau P_h(t)$, fiber i heals up and a new threshold is assigned to it chosen from the distribution given by Eq. (1).

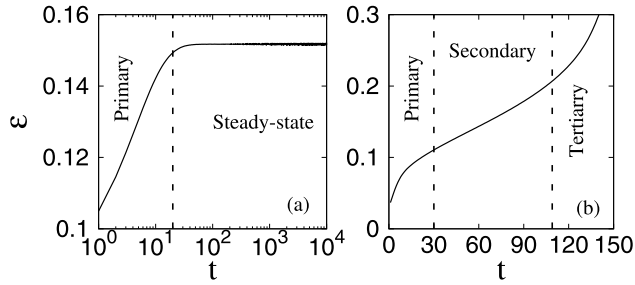


FIG. 1. Typical time evolution of strain for (a) the larger healing rate ($\omega = 0.01$) and (b) the smaller healing rate ($\omega = 0.001$). Other parameters are kept at $k_B T = 0.1$, $\sigma = 0.1$, and $\delta = 0.5$ for both panels.

After inspecting all the fibers in this manner, the number of surviving fibers L_t is updated to $L_{t+\tau}$ and so is the force per fiber.

F. Dimensionless quantities

As discussed above, in this model, the time interval τ is not an arbitrary time step, but rather is the characteristic time for the elementary physical processes in the model: failure and healing of fibers and the subsequent stress relaxation.

In the numerical simulation described in the next section, we adopt the unit system in which $\tau = 1$. The numerical values for the two rate constants (k_1 , ω) are thus expressed in terms of $1/\tau$. The unit of stress is chosen to be $\sqrt{Gk_B T/\Omega}$, and the unit of energy is $k_B T$. Namely, we set $k_B T = 0.1$ and $Gk_B T/\Omega = 0.1$. Among several parameters that affect the dynamics of the present model, we focus on the initial stress σ_0 and the two rate constants: k_1 and ω .

III. NUMERICAL RESULTS

In this study, the model is investigated numerically. The number of fibers N is set to be 10^5 , and the ensemble average is taken over 10^4 samples. The disorder strength, the activation energy, and the applied stress are kept fixed at 0.5, 0.1, and 0.1, respectively.

The time evolution of the system is inspected via strain and strain rate, which are observable in most experiments. Since the total load on the system is kept constant during the simulation, the strain at time t is $\epsilon_t = \sigma_0/\phi_t$, where σ_0 is the initial stress. Since the fraction of intact fibers ϕ_t is a decreasing function of time, the strain ϵ_t is an increasing function of time.

A. Fate of the system

The dynamic behavior of the system is determined by the competition between the two elementary processes: healing and failure. As shown in Fig. 1(a), if the healing process is sufficiently effective (i.e., the healing rate is dominant over the rupture rate), the strain increases with time initially and then saturates at a particular value. This is regarded as the steady state and the system does not fail in this case.

Since the strain in this model remains constant at steady states, one may argue whether the model can represent a

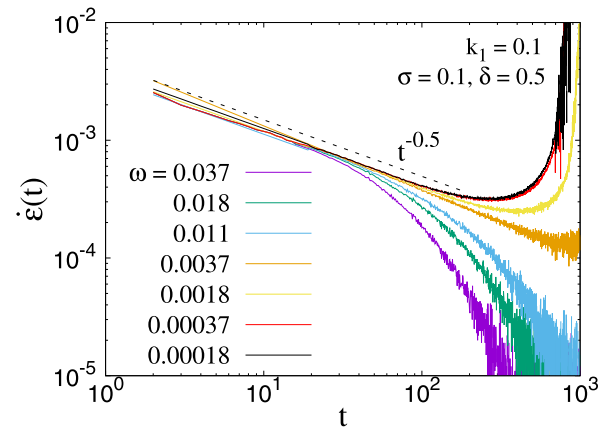


FIG. 2. Variation of the strain rate generated in the bundle with increasing time during the course of failure. k_1 , $k_B T$, σ , and δ are kept fixed at 0.1, 0.1, 0.1, and 0.5, respectively. ω , on the other hand, is varied continuously. Close to a critical value ω_c (≈ 0.0036), we observe $\dot{\epsilon}(t) \sim t^{-p}$, where $p = 0.5$. For $\omega < \omega_c$, the bundle breaks completely, while for $\omega > \omega_c$ it reaches a steady state.

sheared system, in which strain grows indefinitely with time. We would like to point out that the strain in this model represents the *elastic strain*, which is proportional to the stress. Thus, the elastic strain is also finite. It is the *inelastic strain* that grows indefinitely with time, and the total strain is the sum of the elastic strain and the inelastic strain. The inelastic strain is not explicitly modeled here, as it does not involve stress.

If the healing process is not sufficiently effective, the system fails eventually. Time evolution of the strain rate resembles creep rupture, exhibiting three stages as shown in Fig. 1(b).

This qualitative difference in the dynamic behavior is more apparent if the healing rate ω is varied with the rate of rupture k_1 being fixed. This is shown in Fig. 2. For smaller ω , the healing rate is insufficient to stabilize the system, and the system eventually fails after the acceleration of deformation. For larger ω , the healing rate is dominant over the rupture rate. In this case, the strain rate tends to zero quickly. Namely, deformation stops and the system reaches the steady state. At intermediate values of ω , the strain rate appears to decay as a power law, which is eventually cut off at a certain timescale depending on the healing rate ω . The strain rate vanishes quickly for larger ω or increases toward failure for smaller ω .

There seems to exist a critical point ($\omega \rightarrow \omega_c$), at which the strain rate decays in a power-law manner for a long time. In Fig. 3, the power-law behavior continues up to 3 orders of magnitude in time for some values of k_1 . The strain rate is described as $\dot{\epsilon} \propto t^{-p}$, and the exponent $p \simeq 0.5$ in the parameter range investigated here.

B. Critical behavior

The strain rate eventually diverges (breakdown) or vanishes (steady state) depending on the healing rate ω . In Fig. 2, each curve corresponds a different value of ω .

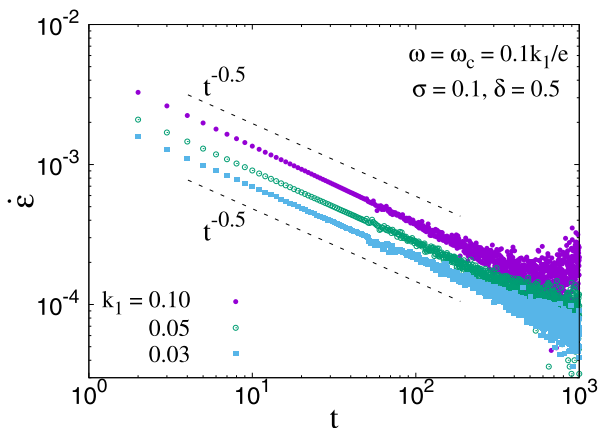


FIG. 3. Behavior of the strain rate at the critical point: $\omega = \omega_c$. For $k_1 = 0.1, 0.05$, and 0.03 , the values of ω_c will be close to $0.0036, 0.0018$, and 0.0011 , respectively. We observe $\dot{\epsilon}(t) \sim t^{-0.5}$ independent of the value of k_1 . $k_B T, \sigma$, and δ are kept constant at $0.1, 0.1$, and 0.5 , respectively.

These behaviors of strain rate $\dot{\epsilon}(t)$ are described in a much simpler manner using a scaling relation:

$$\dot{\epsilon}(t) \propto t^{-p} f_{\pm}(t|\omega - \omega_c|^{\mu}). \quad (6)$$

Here $f(\cdot)_{\pm}$ represents the scaling functions below ($\omega < \omega_c$) or above ($\omega > \omega_c$) the critical state. It thus implies that the strain rate curves at various values of ω collapse on a few branches. Figure 4 shows the collapse of the data onto two branches, which are above or below the critical state. The scaling function at the critical state is constant, and the strain rate is expected to decay as t^{-p} . This is shown in Fig. 3.

In addition, the scaling relation (6) implies the existence of characteristic time that behaves as $|\omega - \omega_c|^{-\mu}$. This can be directly confirmed by calculating the characteristic time from the time series. For ω larger than the critical value ω_c , the relaxation time to the steady state can be defined by fitting the strain rate with the following equation:

$$\dot{\epsilon} \sim (t + c)^{-p} e^{-t/t_0}, \quad (7)$$

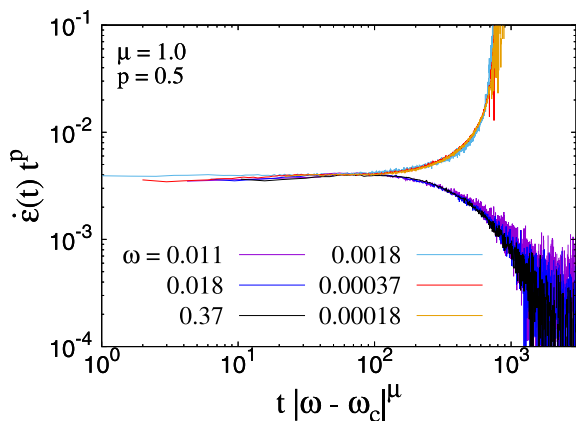


FIG. 4. Collapse of strain rate behaviors at various values of ω with $\mu = 1.0$ and $p = 0.5$. This implies the validity of Eq. (6). k_1 is kept constant at 0.1 .

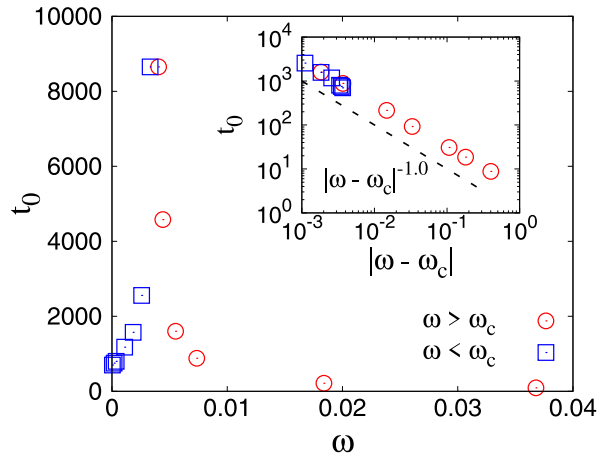


FIG. 5. Behavior of the characteristic time t_0 associated with the time evolution of the strain rate. t_0 is estimated from Eq. (7) in the limit $\omega > \omega_c$. For $\omega < \omega_c$, t_0 is the time required for the model to fail. t_0 diverges around ω_c in a scale-free manner: $t_0 \sim |\omega - \omega_c|^{-\mu}$, where $\mu = 1.0$. This is consistent with Fig. 4 as well as Eq. (6).

where c and t_0 are time constants. This behavior is similar to the Omori-Utsu law [22,23] for the time evolution of the aftershocks rate. Since c involves the initial behavior, the exponential cutoff defines the characteristic time t_0 for relaxation. Similarly, another characteristic time for smaller ω ($\omega < \omega_c$) is defined as the lifetime of the system. This is also denoted by t_0 and is shown in Fig. 5 together with t_0 estimated by Eq. (7) for $\omega > \omega_c$. They both increase toward the critical state, obeying $|\omega - \omega_c|^{-1}$ as shown in Fig. 5. This behavior is consistent with the scaling behavior, Eq. (6).

C. Correlation time for fluctuations in strain

The system reaches the steady state for ω larger than ω_c . The strain ϵ fluctuates around the mean value. In Fig. 6, the time series of strain is shown for the initial 10^4 time steps. The correlation time seems to be longer in Fig. 6(b), where ω is closer to the critical value.

This is quantitatively shown by computing an autocorrelation function, which is shown in Fig. 7. The function can be

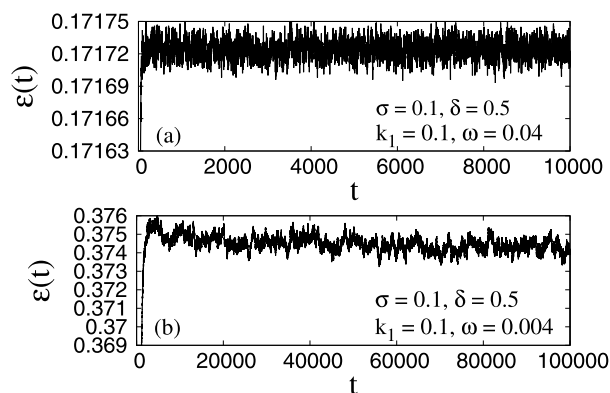


FIG. 6. Strain $\epsilon(t)$ as a function of time t for the region $\omega > \omega_c$. Panels (a) and (b) show the results far away from ω_c and close to ω_c , respectively. We set $k_1 = 0.1, k_B T = 0.1, \sigma = 0.1$, and $\delta = 0.5$.

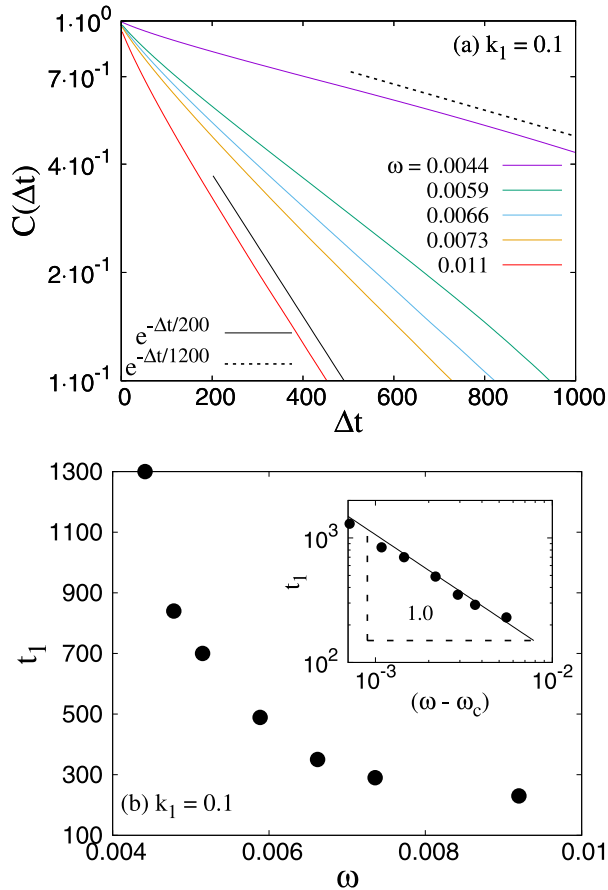


FIG. 7. (a) Correlation function associated with the t vs $\epsilon(t)$ behavior (see Fig. 6) for $k_1 = 0.1$, $k_B T = 0.1$, $\sigma = 0.1$, and $\delta = 0.5$. We observe $C(\Delta t) \sim \exp(-\Delta t/t_1)$. The correlation function is longer closer to ω_c . The inset shows the divergence of t_1 as ω approaches ω_c : $t_1 \sim (\omega - \omega_c)^{-\xi}$, with $\xi = 1.0$, which is the same value as μ .

calculated from n values of ϵ , where n stands for increasing time steps. Since the system breaks down at finite time for $\omega < \omega_c$, the correlation function $C(\Delta t)$ can be computed only for $\omega > \omega_c$, where a steady state is realized. $C(\Delta t)$ has the following form for a series t vs $\epsilon(t)$ in the steady state. n is the number of data points considered to calculate $C(\Delta t)$. $n = 5 \times 10^4$ in our case, after the model is well inside the steady state:

$$C(\Delta t) = \frac{\frac{1}{n} \sum_{t=1}^{n-\Delta t} [\epsilon(t) - \bar{\epsilon}][\epsilon(t + \Delta t) - \bar{\epsilon}]}{\frac{1}{n} \sum_{t=1}^n [\epsilon(t) - \bar{\epsilon}]^2}, \quad (8)$$

where $\bar{\epsilon}$ is given by

$$\bar{\epsilon} = \frac{1}{n} \sum_{t=1}^n \epsilon(t). \quad (9)$$

The correlation function is exponential as shown in Fig. 7(a). We can thus extract the correlation time t_1 by fitting the data with $\exp(-\Delta t/t_1)$. The result is shown in Fig. 7(b), in which the correlation time increases as ω decreases to the critical value ω_c . The behavior suggests the power-law increase of correlation time: $t_1 \propto (\omega - \omega_c)^{-\xi}$. Here the exponent ξ is estimated as 1.0, which is the same value as exponent μ . Both the time constants appear to increase toward the critical point with similar exponents.

IV. DISCUSSIONS

We have studied the fiber bundle model at a finite temperature with a healing mechanism. The temperature, in our case, helps both the rupture and the healing process. Rich relaxation dynamics is observed due to the interplay of the above two factors. The model is mostly observed for different healing rate constants while other parameters are kept fixed.

In the presence of both probabilistic rupture and infinite healing, the model either stabilizes or meets global failure depending on whether the healing rate constant is higher or lower. In the former case, the strain (or strain rate), generated in the model with time, shows a primary creep followed by a steady state, while for the latter case, all three creep stages, primary, secondary and tertiary, are observed. In the case where the steady state is realized, the strain rate shows the Omori-Utsu-like behavior with an exponent which is insensitive to the rate of probabilistic failure.

The critical healing rate, which is a function of the rate of probabilistic failure, is observed to divide the strain rate in two branches: towards the steady state or towards global failure, in a well-defined scaling rule. As the healing rate approaches its critical value, the correlation time associated with the time evolution of strain diverges in a scale-free manner.

ACKNOWLEDGMENTS

S.R. is supported by the Research Council of Norway through its Centres of Excellence funding scheme, Project No. 262644. T.H. is supported by Japan Society for the Promotion of Science (JSPS) Grants-in-Aid for Scientific Research (KAKENHI), Grants No. 16H06478 and No. 19H01811.

[1] B. K. Chakrabarti and L. G. Benguigui, *Statistical Physics of Fracture and Breakdown in Disordered Systems* (Oxford University, Oxford, 1997).
 [2] H. J. Herrmann and S. Roux, *Statistical Models for the Fracture of Disordered Media* (North-Holland, Amsterdam, 1990).
 [3] A. G. Duba, W. B. Durham, J. W. Handin, and H. F. Wang, *The Brittle-Ductile Transition in Rocks*, Geophysical Monograph Series (American Geophysical Union, Washington, DC, 2013).

[4] H. Nechad, A. Helmstetter, R. El Guerjouma, and D. Sornette, Andrade and critical time-to-failure laws in fiber-matrix composites: Experiments and model, *J. Mech. Phys. Solids* **53**, 1099 (2005).
 [5] H. Nechad, A. Helmstetter, R. El Guerjouma, and D. Sornette, Creep Ruptures in Heterogeneous Materials, *Phys. Rev. Lett.* **94**, 045501 (2005).
 [6] E. Rabinowicz, *Friction and Wear of Materials*, 2nd ed. (Wiley & Sons, New York, 2013).

- [7] M. Schneebeli, Numerical simulation of elastic stress in the microstructure of snow, *Ann. Glaciol.* **38**, 339 (2004).
- [8] F. T. Pierce, 32-X.-Tensile tests for cotton yarns v.—“the weakest link” theorems on the strength of long and of composite specimens, *J. Text. Inst. Trans.* **17**, 355 (1926).
- [9] H. E. Daniels, The statistical theory of the strength of bundles of threads, *Proc. R. Soc. London, Ser. A* **183**, 405 (1945).
- [10] A. Hansen, P. C. Hemmer, and S. Pradhan, *The Fiber Bundle Model: Modeling Failure in Materials* (Wiley-VCH, Weinheim, 2015).
- [11] S. Pradhan and P. C. Hemmer, Relaxation dynamics in strained fiber bundles, *Phys. Rev. E* **75**, 056112 (2007).
- [12] N. Yoshioka, F. Kun, and N. Ito, Kertész line of thermally activated breakdown phenomena, *Phys. Rev. E* **82**, 055102(R) (2010).
- [13] N. Yoshioka, F. Kun, and N. Ito, Time evolution of damage in thermally induced creep rupture, *Europhys. Lett.* **97**, 26006 (2012).
- [14] S. Roy and T. Hatano, Creeplike behavior in athermal threshold dynamics: Effects of disorder and stress, *Phys. Rev. E* **97**, 062149 (2018).
- [15] S. Roy and T. Hatano, Creep failure in a threshold-activated dynamics: Role of temperature during a subcritical loading, *Phys. Rev. Research* **2**, 023104 (2020).
- [16] B. R. Lawn, *Fracture of Brittle Solids* (Cambridge University, Cambridge, England, 1993).
- [17] B. D. Coleman, Statistics and time dependence of mechanical breakdown in fibers, *J. Appl. Phys.* **29**, 968 (1958).
- [18] R. Scorretti, S. Ciliberto, and A. Guarino, Disorder enhances the effects of thermal noise in the fiber bundle model, *Europhys. Lett.* **55**, 626 (2001).
- [19] S. Roux, Thermally activated breakdown in the fiber-bundle model, *Phys. Rev. E* **62**, 6164 (2000).
- [20] S. Pradhan and B. K. Chakrabarti, Failure due to fatigue in fiber bundles and solids, *Phys. Rev. E* **67**, 046124 (2003).
- [21] I. Reiweger, J. Schweizer, J. Dual, and H. J. Herrmann, Modelling snow failure with a fibre bundle model, *J. Glaciol.* **55**, 194 (2009).
- [22] F. Omori, On the aftershocks of earthquakes, *J. Coll. Sci., Imperial Univ. Tokyo* **7**, 111 (1894).
- [23] T. Utsu, Aftershocks and earthquake statistics (3): Analyses of the distribution of earthquakes in magnitude, time and space with special consideration to clustering characteristics of earthquake occurrence (1), *J. Fac. Sci., Hokkaido Univ., Series 7: Geophysics* **3**, 379 (1972).